



MoSET1-dependent transcription factors regulate different stages of infection-related morphogenesis in *Pyricularia oryzae*

Minh, Dang Ngoc
Tsukahara, Yusaku
Thach, Dang An
Ikeda, Ken-ichi
Nakayashiki, Hitoshi

(Citation)

Journal of General Plant Pathology, 89(2):77-83

(Issue Date)

2023-03

(Resource Type)

journal article

(Version)

Accepted Manuscript

(Rights)

This version of the article has been accepted for publication, after peer review (when applicable) and is subject to Springer Nature's AM terms of use, but is not the Version of Record and does not reflect post-acceptance improvements, or any corrections. The Version of Record is available online at:...

(URL)

<https://hdl.handle.net/20.500.14094/0100479376>



MoSET1-dependent transcription factors regulate different stages of infection-related morphogenesis in *Pyricularia oryzae*

Authors, Dang Ngoc Minh*, Yusaku Tsukahara*, Dang An Thach, Ken-ich Ikeda, Hitoshi Nakayashiki**

Graduate School of Agricultural Science, Kobe University, 1-1 Rokkodai-cho, Nada, 657-8501 Kobe, Japan

*These two authors contributed equally to this work.

**Address for correspondence: Hitoshi Nakayashiki. Laboratory of cell function and structure, Graduate School of Agricultural Science, Kobe University, 1-1 Rokkodai-cho, Nada, 657-8501 Kobe, Japan. Phone & Fax : +81-78-803-5867 ; email : hnakaya@kobe-u.ac.jp

Total text pages:23

The numbers of tables and figures: 0 table and 5 figures

1 Abstract

2

3 MoSET1, an H3K4 histone methyltransferase in *Pyricularia oryzae* plays a key role in
4 infection-related morphogenesis of the fungus. Our previous study identified approximately
5 400 genes whose expression were possibly regulated directly by MoSET1 during appressorium
6 formation. In this study, we focused on five such MoSET1-dependent transcription factors (TF)
7 whose mRNA expression was induced during infection. A gene deletion approach was used for
8 three of the five TF genes (MGG_04699, MGG_06898, and MGG_07450) while a gene
9 silencing technique was applied to the remaining two genes (MGG_00472 and MGG_07386)
10 due to the difficulty in constructing a gene deletion mutant. The phenotypic characterization of
11 the gene knock-out and -down mutants revealed that MGG_06898 played a crucial role in
12 sporulation, MGG_04699 were involved in appressorium formation, and MGG_00472 and
13 MGG_04699 were required for the full virulence of the fungus. These results demonstrated
14 that MoSET1 contributes to the pathogenicity of the fungus by controlling transcription factors
15 that further regulate different steps in the infection process of *P. oryzae*

16

17

18

19 **Key words:** *Pyricularia oryzae*, transcription factor, histone methylation

20 Introduction

21

22 The filamentous fungus *Pyricularia oryzae* (synonym: *Magnaporthe oryzae*) causes
23 blast disease on various gramineous plants such as rice, wheat, oat and so on (Kato et al., 2000).
24 The blast fungus shows drastic morphological changes during the infection cycle (Talbot, 2003).
25 Following attachment on the host leaf surface, a spore germinates and forms an appressorium
26 at the tip of the germ tube. At the base of the appressorium, a penetration pore and peg are
27 formed to colonize a host cell with infection hyphae. These morphological changes are
28 accompanied with remarkable changes in gene expression (Jeon et al., 2020) that may involve
29 cell type-specific epigenetic control of chromatin structure.

30 Epigenetics describes heritable changes in gene expression caused by non-genetic
31 mechanisms such as chemical modifications of DNA, RNA and histone protein as well as
32 regulations by non-coding RNAs (Aristizabal et al., 2019). Histone methylation is a process
33 that methyl groups are added to lysine or arginine in histone proteins. Both histone arginine
34 methyltransferases (RMTs) and lysine methyltransferases (KMTs) catalyze the transfer of
35 methyl groups from *S*-adenosyl methionine to core histone proteins. In *P. oryzae*, gene deletion
36 analysis of eight possible KMTs revealed that MoSET1 responsible for H3K4 methylation
37 plays a pivotal role in infection-related morphogenesis of the fungus (Pham et al., 2015a). Loss
38 of MoSET1 led to a deficiency in cell growth, sporulation, appressorium formation, production
39 of cell wall degradation enzymes, and pathogenicity (Pham et al., 2015a, b; Vu et al., 2013).
40 RNA-seq analysis suggested that approximately 2,000 genes were up- or down-regulated
41 during appressorium formation in a MoSET1-dependent manner. However, ChIP-seq analysis
42 of MoSET1 protein revealed that only approximately 400 of the MoSET1-dependent genes
43 were directly regulated by MoSET1 (Pham et al., 2015a), suggesting the involvement of a
44 signaling cascade starting from MoSET1. In fact, the 400 genes contained possible signal
45 mediators such as transcription factors (TFs) and kinases.

46 In this study, we focused on MoSET1-dependent TFs. In fungi, TFs are key players in
47 the signal transduction pathways and regulatory mechanisms (Shelest, 2008). For instance,
48 Gomi and his coworkers (2000) stated that the deletion of AmyR, a zinc binuclear cluster DNA-
49 binding protein in the Gal4p TF family, led to a decrease in amylolytic enzyme activities and
50 vegetative growth of *Aspergillus oryzae* on starch medium. In *Parastagonospora nodorum*,
51 PnPf2, a TF belonging to the Zn2-Cys6 zinc finger subfamily positively regulated necrotrophic
52 effector proteins and played an important role in the virulence on wheat (Jones et al., 2019). In

53 *P. oryzae*, systematic analyses of the Zn²-Cys₆ TF family and the Cys₂-His₂ zinc finger TF
54 family were conducted (Cao et al., 2016; Lu et al., 2014) to reveal that 61 of 104 Zn²-Cys₆
55 TFs and 44 of 47 Cys₂-His₂ TFs were involved fungal development and infection-related
56 morphogenesis such as growth, conidiation, appressorium formation and pathogenicity (Cao et
57 al., 2016; Lu et al., 2014). Among the 22 Cys₂-His₂ TFs required for the full virulence of the
58 fungus, 2 were MoSET1-dependent TFs.

59 Here we carried out the functional analysis of five MoSET1-dependent TFs to explore
60 their roles in the pathogenicity of *P. oryzae*. The results suggested that MoSET1 orchestrates
61 various TFs to achieve successful infection of host plants with *P. oryzae*.

62

63 **Materials and methods**

64

65 **Fungal strains and host plants**

66 The wheat-infecting *P. oryzae* strain Br48 was collected in Brazil (Urashima et al.,
67 1999). Fungal strains were preserved on barley seed media at 4°C for long-term storage, and
68 cultured on potato dextrose agar (PDA) at 25°C for working stock. “Norin 4” (N4), a cultivar
69 of common wheat (*Triticum aestivum* L.) was used as a host plant of the Br48 strain.

70 **Construction of gene knock-out and -down mutants**

71 The split-maker disruption method (Catlett et al., 2003) was applied to construct
72 deletion mutant strains (Fig. S1). First, up- and down-stream flanking regions of a target gene
73 were amplified by PCR using KOD-Plus-Neo polymerase (TOYOBO, Osaka, Japan) and
74 individually cloned by blunt-end ligation at PvuII and EcoRV sites of pSP72-hph containing a
75 hygromycin B phosphotransferase gene (Hph) (Morita et al., 2013). Using the resulting
76 plasmids, two DNA fragments containing a part of Hph and the flanking genomic region were
77 amplified by PCR using KOD-Plus-Neo polymerase as shown in Fig. S1. The PCR products
78 were purified using Wizard SV Gel and PCR Clean-up System (Promega, Madison, WI, USA)
79 after agarose gel electrophoresis, and used for fungal transformation. A list of primers used to
80 amplify the genomic fragments was given in Table S1.

81 A retrotransposon-based gene silencing vector, pSilent-MG (Vu et al., 2011) was used
82 to generate gene knock-down mutants. A target fragment was amplified by PCR using KOD-
83 Plus-Neo polymerase and a pair of specific primers (Table S1), and inserted at a BglIII site in
84 pSilent-MG.

85 To obtain fungal transformants with a gene disruption or silencing vector, a PEG-
86 mediated transformation method was used as described previously (Nakayashiki et al., 1999).
87 The resulting fungal transformants having a gene disruption at the desired genomic location or
88 a silencing vector were screened by PCR with appropriate sets of primers for each target gene
89 (Fig. S1, Table S1).

90 To construct a gene complementation strain, a genomic DNA fragment containing a
91 target gene and its surrounding region was amplified by PCR with sets of specific primers
92 (Table S1) and KOD One (TOYOBO). The PCR product was introduced into the corresponding
93 gene deletion mutant through PEG-mediated co-transformation with the marker plasmid pII99

94 carrying a geneticin-resistant cassette. Presence or absence of a target gene in the transformants
95 was checked by PCR using a pair of primers (Table S1) in the coding sequence (Fig. S1).

96 **Phenotypic characterization of gene knock-out and -down mutants**

97 Every phenotypic assay was performed with three biological replicates unless mentioned
98 otherwise.

99 ***1. Vegetative growth***

100 A mycelial plug was placed at the center of CM agar medium (0.3% casamino acids,
101 0.3% yeast extract, 0.5% sucrose, 0.5% agar) and cultured at 25°C. The colony diameter was
102 measured at 9 days after incubation.

103 ***2. Conidiation, conidial germination, and appressorium formation***

104 Fungal strains were cultured on oatmeal agar media and incubated at 25°C for 7 days,
105 and then, aerial mycelia were removed using the tip of a 1.5 ml microtube. The fungal strains
106 were further cultured under blacklight blue (BLB) light for 3 days. Conidial suspension was
107 prepared by adding 10 ml of distilled water per plate to fungal culture as described previously
108 (Hyon et al., 2012). For germination and appressorium formation assay, 10 µl conidial
109 suspension (12×10^5 conidia/ml) were dropped on a cover glass and incubated at 25°C in the
110 dark under a high humidity condition. Conidial germination was observed after 5 h incubation,
111 and the rate of appressorium formation was counted after 8, 12, 24 h incubation. At least 100
112 conidia were observed to calculate the rates of conidial germination and appressorium
113 formation in each replicate.

114 ***3. Plant infection assay***

115 Seeds of the wheat cultivar Norin 4 were sown in vermiculite supplied with Hyponex
116 (Hyponex Japan, Osaka, Japan) in plastic seedling pots (5.5 cm × 15 cm × 10 cm), and grown
117 in a plant growth chamber at 23°C with a 12 h-photoperiod for 8 days. Tween 20 (0.01%) was
118 added to conidia suspension, and sprayed onto the adaxial side of the 8-day-old primary wheat
119 leaves. The inoculated seedlings were incubated in a dark and high humidity box for 24 h, and
120 then moved to a plant growth chamber at 23°C with a 12 h-photoperiod for 4-5 days. The
121 disease symptoms were graded by a combination of lesions size (0 to 5) and color (brown [B]
122 or green [G]) as described previously (Hyon et al., 2012). 0, no visible lesion; 1, pinpoint
123 spots; 2, small size (< 1.5 mm); 3, intermediate size (< 3 mm); 4, large and typical blast lesion;
124 5, whole blighting of leaf blades.

125 Cytological assay

126 Cytological observation was performed as described by Hyon et al. (2012) with a slight
127 modification. The inoculated leaves were collected for observation of appressorium formation
128 at 12 hpi and of infection hyphae in host cells at 24 hpi. The samples were bleached by deeply
129 boiled in alcoholic lactophenol (lactic acid/phenol/glycerol/distilled water/ethanol, 1:1:1:1:8 in
130 volume) at 98°C for 5 min. Then, microscopic observation was performed using an
131 epifluorescent microscope under bright and fluorescent fields.

132 RNA isolation and qRT-PCR analysis

133 For RNA extraction, approximately, 50-120 mg of vegetative mycelia, spores or
134 infected leaves were ground to a fine powder in liquid nitrogen with a mortar and pestle. Total
135 RNA was isolated from frozen samples using Sepasol RNA I Super G (Nacalai Tesque, Kyoto,
136 Japan). Total RNA was further cleaned up using the NucleoSpin RNA Clean-up Kit (Macherey-
137 Nagel, Düren, Germany) following manufacture's instruction.

138 For RT-qPCR analysis, 1 µg of total RNA was subjected to cDNA synthesis using the
139 ReverTra Ace qPCR RT Master Mix with gDNA Remover kit (TOYOBO). RT-qPCR assay
140 was carried out with GeneAce SYBR qPCR Mix α (Nippon Gene, Tokyo, Japan) using pairs
141 of primers listed in Table S1. The actin gene (MGG_03982) was used as an internal control.
142 The level of target mRNA, relative to the mean of the internal control was calculated by the
143 comparative Ct method.

144

145 **Results**

146

147 **Transcriptional analysis of MoSET1-dependent TFs during plant infection by *P. oryzae***

148 Among approximately 400 genes that were potentially regulated directly by MoSET1
149 (Pham et al., 2015a), 18 genes exhibited a typical characteristic of TFs. In this study, we chose
150 5 of the 18 putative TFs, MGG_00472, MGG_04699, MGG_06898, MGG_07386 and
151 MGG_07450 for functional analysis. First, to gain insight into the functions of these TFs, their
152 gene expression profile at hyphal, conidial and infectious stages was examined by qRT-PCR.
153 At the conidial stage, the mRNA abundance of MGG_04699, MGG_07386 and MGG_07450
154 was decreased while that of MGG_06898 was significantly increased compared to the hyphal
155 stage (Fig. 1). Interestingly, the expression of the MoSET1-dependent TFs was generally
156 increased in infection stages relative to the hyphal stage, especially at an early stage (5 hpi).
157 The abundance of MGG_04699 and MGG_06898 mRNA was increased by approximately 8-
158 fold and 16-fold, respectively, at 5 hpi (Fig. 1). In contrast, the mRNA abundance of
159 MGG_07386 was significantly decreased at 5 hpi but increased later at 12 hpi (Fig. 1). These
160 results were consistent with the idea that these TFs play roles in the infection process of *P.*
161 *oryzae*.

162

163 **Gene silencing of MGG_00472 and MGG_07386**

164 Despite several trials, we were not able to obtain a gene deletion mutant of MGG_00472
165 or MGG_07386. This might be due to a lethality of the gene deletion mutants. Indeed, the
166 knock-out mutant of NCU00116, the ortholog of MGG_00472 in *Neurospora crassa*, is
167 maintained only in the form of a heterokaryon (Chen et al., 1998;
168 https://www.fgsc.net/fgsc/strain_detail.php?OrgID=22094). Thus, we decided to use pSilent-
169 MG to analyze the function of MGG_00472 and MGG_07386. pSilent-MG is a gene silencing
170 vector that triggers retrotransposon-induced gene silencing. In this system, a target gene
171 fragment inserted at a cloning site in the LTR-retrotransposon MAGGY induces both
172 transcriptional and post-transcriptional gene silencing together with the element in *P. oryzae*
173 (Vu et al., 2011).

174 After initial screening, two candidate transformants each for MGG_00472 or
175 MGG_07386 were subjected to qRT-PCR analysis to assess levels of gene silencing. The
176 candidates showed silencing of the target gene at varying degrees in vegetative mycelia (Fig.

177 2). Consequently, the transformants, KD_mgg00472-12 and KD_mgg07386-13, were selected
178 for further phenotypic analyses.

179

180 **Phenotypic characterization of gene knock-out and -down mutants of MoSET1-** 181 **dependent TFs**

182 Three gene knock-out mutants, Δ mgg_04699, Δ mgg_06898 and Δ mgg_07450, and two
183 knock-down mutants, KD_mgg00472-12 and KD_mgg07386-13 were subjected to phenotypic
184 analyses with respect to growth, sporulation, germination, appressorium formation, and
185 pathogenicity on the host plant.

186 First, the growth rates of the mutants on rich media (CM agar media) were assessed.
187 Δ mgg_04699, Δ mgg_06898, and KD_mgg00472-12 showed a slower growth while,
188 interestingly, the growth rate of KD_mgg07386-13 was a little faster than the WT strain (Fig.
189 3a).

190 With an exception of Δ mgg_07450, all the mutant examined displayed a decrease in
191 conidiation compared to WT at varying degrees (Fig. 3b). Especially, Δ mgg_06898 produced
192 almost no conidia, suggesting that MGG_06898 plays a crucial role in conidiogenesis in *P.*
193 *oryzae*. Meanwhile, due to this, further phenotypic assays that use conidia were not applicable
194 to Δ mgg_06898.

195 The rates of germination and appressorium formation were assessed using conidial
196 suspension dropped on a cover glass. The conidia were incubated in the dark at 25°C up to 24
197 h. The germination rates of the mutants did not differ much from that of WT except that
198 Δ mgg_04699 exhibited a rate less than 60% relative to WT (Fig 3c). In addition, only
199 Δ mgg_04699 showed a deficiency in appressorium formation. At 24 hpi, approximately 50%
200 of conidia formed an appressorium in Δ mgg_04699 while more than 90% of conidia did it in
201 the WT and other mutant strains (Fig. 3d). The deficiency of Δ mgg_04699 in germination and
202 appressorium formation was restored to the WT levels in the gene complementation strain,
203 indicating that MGG_04699 is responsible for the phenotypic alterations in the mutant.

204 In infection assay, KD_mgg00472-12 and Δ mgg_04699 showed significantly reduced
205 virulence on the host plant (Fig. 4a). The infection types of KD_mgg00472-12 and
206 Δ mgg_04699 were 3-4BG and 23BG, respectively. Cytological observation of infected leaves
207 indicated that both KD_mgg00472-12 and Δ mgg_04699 exhibited a delay in invasion to plant
208 cells compared to WT. At 24 hpi, the rates of appressoria that successfully formed infection
209 hyphae in the host cell were 45% and 31% with KD_mgg00472-12 and Δ mgg_04699,

210 respectively, while that with WT were approximately 80% (Fig. 4b). These results suggested
211 that MGG_00472 and MGG_04699 contributed to the full virulence of *P. oryzae* by regulating
212 their downstream genes.

213 The infection type of KD_mgg07386-13 was 5B. Lesions appeared in almost the whole
214 leave (Fig. 4a). However, in contrast to leaves infected with the WT strain, the color of lesions
215 was mostly brown, indicating that this mutant induced more resistant reaction than did the WT
216 strain. Thus, MGG_07386 may be required for suppressing a part of resistant reactions by the
217 host plant.

218

219 Discussion

220 Among the MoSET1-dependent TFs examined in this study, MGG_00472 and
 221 MGG_04699 considerably contributed to the virulence of *P. oryzae*. MGG_04699 named as
 222 MoFLBC (Cao et al., 2016) is a homolog of FlbC, C2H2 transcription factor in *Aspergillus*
 223 *nidulans* (Kwon et al., 2010). FlbC is necessary for conidiation, conidial germination and,
 224 proper development in *A. nidulans*. Possible orthologs of FlbC were present in a wide range of
 225 fungal species. In *Fusarium verticillioides*, the FlbC ortholog negatively regulated the
 226 production of conidia (Malapi-Wight et al., 2014). More recently, Boni et al. (2018) reported
 227 that FLB-3, an ortholog of FlbC in *Neurospora crassa*, was essential for fungal development.
 228 Thus, FlbC homologs play roles in regulating various stages of fungal development in a wide
 229 range of ascomycetes.

230 In *P. oryzae*, Cao et al. (2016) showed that a deletion mutant of MGG_04699 had a severe
 231 defect in sporulation and its virulence to the host plant as shown in this study. However,
 232 contrary to our study, the rates of germination and appressorium formation were 96.9% and
 233 94.9%, respectively, relative to WT in their study. This apparent discrepancy may be due to a
 234 difference in the strains and/or experimental conditions.

235 To date, MGG_00472 as well as MGG_07386 and MGG_07450, have not been well-
 236 characterized in *P. oryzae*. MGG_00472 is an ortholog of the *Aab-1* gene of *N. crassa*
 237 (NCU00116) encoding a CCAAT-binding TF subunit. *Aab-1* was reported to regulate a
 238 glutamate dehydrogenase gene and have pleiotropic effects on growth and development (Chen
 239 et al., 1998). Consistently, KD_mgg00472-12 showed defects in growth, sporulation, and
 240 virulence to the host plant. Thus, MGG_00472 may also have pleiotropic effects on growth and
 241 development in *P. oryzae*. Possible orthologs of MGG_07386 and MGG_07450 were
 242 conserved in ascomycete fungi but their biological functions were so far not well-understood.

243 MGG_06898, namely MoMyb1, encodes a TF belonging to the Myb protein family.
 244 Consistent with our results, Dong et al. (2015) previously revealed that a deletion mutant of
 245 MoMyb1 showed defects in vegetative growth, conidiation and conidiophore development. In
 246 the MoMyb1 deletion mutant, several conidiogenesis-related genes such as MoMSN2, MoFlbC
 247 (MGG_04699), MoGLUS, MoSTUA, and MoCON8 were significantly down-regulated (Dong
 248 et al., 2015). Thus, MoSET1-dependent MoMyb1 plays a key role in conidiogenesis.

249 Based on the literatures and this work, at least fifteen MoSET1-dependent TF genes in
 250 *P. oryzae* have been characterized to date, which includes MGG_00472, MGG_07386,
 251 MGG_07450, MGG_01414 (Xlr1), MGG_01518 (MoNIT4), MGG_01486 (FZC2),

252 MGG_02880 (FZC9), MGG_04699 (MoFLBC), MGG_06898 (MoMyb1), MGG_08199
253 (FAR2), MGG_09200 (TDG1), MGG_09950 (FZC54), MGG_00617 (MoVOSA),
254 MGG_01734, and MGG_13778 (MoGIS2) (Cao et al., 2016; Dong et al., 2015; Kim et al.,
255 2014; Lu et al., 2014). Among those, three (MGG_00472, MGG_06898, MGG_09950), ten
256 (MGG_00472, MGG_01518, MGG_01486, MGG_02880, MGG_04699, MGG_06898,
257 MGG_08199, MGG_09200, MGG_01734, MGG_07386), two (MGG_01486, MGG_04699),
258 and four (MGG_00472, MGG_04699, MGG_09200, MGG_13778) TFs were shown to play a
259 role in vegetative growth, sporulation, appressorium formation and virulence to the host plant,
260 respectively (Fig. 5). Thus, MoSET1 may function as a key regulator of the pathogenicity of *P.*
261 *oryzae* by controlling TFs that further regulate various steps in the infection process such as
262 sporulation, appressorium formation, and invasion to the host cell.

263

264 **Acknowledgements**

265 This work was supported by a Grant-in-Aid for Scientific Research (B) from the Japan Society
266 for the Promotion of Science (#25292028 and 16H04883).

267

268 **Declarations**

269 **Conflict of interest** The authors have no conflicts of interest to declare.

270 **Human and animal rights** This article does not contain any studies with human participants
271 or animals performed by any of the authors.

272

273

274

275 **References**

- 276 Aristizabal MJ, Anreiter I, Halldorsdottir T, Odgers CL, McDade TW, Goldenberg A,
 277 Mostafavi S, Kobor MS, Binder EB, Sokolowski MB, O'Donnell KJ (2019) Biological
 278 embedding of experience: A primer on epigenetics. *Proc Natl Acad Sci USA* 117:23261-
 279 23269
- 280 Boni AC, Ambrosio DL, Cupertino FB, Montenegro-Montero A, Freitas FZ, Corrocher FA,
 281 Goncalves RD, Yang A, Weirauch MT, Hughes TR, Larrondo LF, Bertolini MC (2018)
 282 *Neurospora crassa* developmental control mediated by the FLB-3 transcription factor.
 283 *Fungal Biol* 122:570-582
- 284 Cao H, Huang P, Zhang L, Shi Y, Sun D, Yan Y, Liu X, Dong B, Chen G, Snyder JH, Lin F, Lu
 285 J (2016) Characterization of 47 Cys2-His2 zinc finger proteins required for the
 286 development and pathogenicity of the rice blast fungus *Magnaporthe oryzae*. *New*
 287 *Phytol* 211:1035-1051
- 288 Catlett NL, Lee B, Yoder OC, Turgeon BG (2003) Split-marker recombination for efficient
 289 targeted deletion of fungal genes. *Fungal Genetics Reports* 50:9-11
- 290 Chen H, Crabb JW, Kinsey JA (1998) The *Neurospora aab-1* gene encodes a CCAAT binding
 291 protein homologous to yeast HAP5. *Genetics* 148:123-130
- 292 Dong Y, Zhao Q, Liu X, Zhang X, Qi Z, Zhang H, Zheng X, Zhang Z (2015) MoMyb1 is
 293 required for asexual development and tissue-specific infection in the rice blast fungus
 294 *Magnaporthe oryzae*. *BMC Microbiol* 15: 37
- 295 Gomi K, Akeno T, Minetoki T, Ozeki K, Kunagai C, Okazaki N, Iimura Y (2000) Molecular
 296 cloning and characterization of a transcriptional activator gene, *amyR*, involved in the
 297 amylolytic gene expression in *Aspergillus oryzae*. *Biosci Biotechnol Biochem* 64:816-
 298 827
- 299 Hyon GS, Nga NTT, Chuma I, Inoue Y, Asano H, Murata N, Kusaba M, Tosa Y (2012)
 300 Characterization of interactions between barley and various host-specific subgroups
 301 of *Magnaporthe oryzae* and *M. grisea*. *J Gen Plant Pathol* 78:237-246
- 302 Jeon J, Lee GW, Kim KT, Park SY, Kim S, Kwon S, Huh A, Chung H, Lee DY, Kim CY, Lee
 303 YH (2020) Transcriptome profiling of the Rice blast fungus *Magnaporthe oryzae* and
 304 its host *Oryza sativa* during infection. *Mol Plant Microbe Interact* 33:141-144
- 305 Jones DAB, John E, Rybak K, Phan HTT, Singh KB, Lin SY, Solomon PS, Oliver RP, Tan
 306 KC (2019) A specific fungal transcription factor controls effector gene expression and

- 307 orchestrates the establishment of the necrotrophic pathogen lifestyle on wheat. *Sci*
308 *Rep* 9:15884
- 309 Kato H, Yamamoto M, Yamaguchi-Ozaki T, Kadouchi H, Iwamoto Y, Nakayashiki H, Tosa Y,
310 Mayama S, Mori N (2000) Pathogenicity, mating ability and DNA restriction fragment
311 length polymorphisms of *Pyricularia* populations isolated from Gramineae,
312 Bambusideae and Zingiberaceae plants. *J Gen Plant Pathol* 66:30-47
- 313 Kim HJ, Han JH, Kim KS, Lee YH (2014) Comparative functional analysis of the velvet gene
314 family reveals unique roles in fungal development and pathogenicity in *Magnaporthe*
315 *oryzae*. *Fungal Genet Biol* 66:33-43
- 316 Kwon NJ, Garzia A, Espeso EA, Ugalde U, Yu JH (2010) FlbC is a putative nuclear C2H2
317 transcription factor regulating development in *Aspergillus nidulans*. *Mol Microbiol*
318 77:1203-1219
- 319 Lu J, Cao H, Zhang L, Huang P, Lin F (2014) Systematic analysis of Zn2Cys6 transcription
320 factors required for development and pathogenicity by high-throughput gene knockout
321 in the rice blast fungus. *PLoS Pathog* 10:e1004432
- 322 Malapi-Wight M, Kim JE, Shim WB (2014) The N-terminus region of the putative C2H2
323 transcription factor Adal harbors a specie-specific activation motif that regulates
324 asexual reproduction in *Fusarium verticillioides*. *Fungal Genet Biol* 62:25-33
- 325 Morita Y, Hyon G, Hosogi N, Miyata N, Nakayashiki H, Muranaka Y, Inada N, Park P, Ikeda
326 K (2013) Appressorium-localized NADPH oxidase B is essential for aggressiveness and
327 pathogenicity in the host-specific, toxin-producing fungus *Alternaria alternata*
328 Japanese pear pathotype. *Mol Plant Pathol* 14:365-378
- 329 Nakayashiki H, Kiyotomi K, Tosa Y, Mayama S (1999) Transposition of the retrotransposon
330 MAGGY in heterologous species of filamentous fungi. *Genetics* 153:693-703
- 331 Pham KTM, Inoue Y, Vu BV, Nguyen HH, Nakayashiki T, Ikeda K, Nakayashiki H (2015a)
332 MoSET1 (histone H3K4 methyltransferase in *Magnaporthe oryzae*) regulates global
333 gene expression during infection-related morphogenesis. *PLoS Genet* 11:e1005385
- 334 Pham KTM, Nguyen HH, Murai T, Chuma I, Tosa Y, Nakayashiki H (2015b) Histone H3K4
335 methyltransferase globally regulates substrate-dependent activation of cell-wall-
336 degrading enzymes in *Magnaporthe oryzae*. *J Gen Plant Pathol* 81: 127-130
- 337 Shelest E (2008) Transcription factors in fungi. *FEMS Microbiology Letters* 286:145-151

- 338 Talbot NJ (2003) On the trail of a cereal killer: exploring the biology of *Magnaporthe*
339 *grisea*. *Ann Rev in Microbiol* 57:177-202
- 340 Urashima AS, Hashimoto Y, Don LD, Kusaba M, Tosa Y, Nakayashiki H, Mayama S (1999)
341 Molecular analysis of the wheat blast population in Brazil with a homolog of
342 retrotransposon MGR583. *Ann Phytopathol Soc Jpn* 65:429-436
- 343 Vu BV, Takino M, Murata T, Nakayashiki H (2011) Novel vectors for retrotransposon induced
344 gene silencing in *Magnaporthe oryzae* . *J Gen Plant Pathol* 77:147-151
- 345 Vu BV, Pham KT, Nakayashiki H (2013) Substrate-induced transcriptional activation of the
346 MoCel7C cellulase gene is associated with methylation of histone H3 at lysine 4 in the
347 rice blast fungus *Magnaporthe oryzae*. *Appl Environ Microbiol* 79:6823-6832
- 348
- 349

350 **Figure legends**

351

352 **Fig. 1** Quantitative RT-PCR analysis of five MoSET1-dependent transcription factors
 353 at hyphal, conidial and infectious stages in *P. oryzae*. Actin was used to normalize
 354 mRNA expression level. Data show fold change (relative to mRNA quantity in hyphae)
 355 \pm standard error (n = 3). Asterisks are given to indicate significant difference at $p < 0.05$
 356 (*) and $p < 0.01$ (**) (two-tailed *t*-test).

357

358 **Fig. 2** Quantitative RT-PCR analysis of MGG_00472 and MGG_07386 mRNA in
 359 candidates of their knock-down mutants. Actin was used to normalize mRNA
 360 expression level. Data show fold change (relative to mRNA quantity in the wild-type
 361 strain) \pm standard error (n = 3). Different characters indicate significant differences by
 362 Tukey's HSD ($p < 0.05$).

363

364 **Fig. 3** Phenotypic characterization of knock-out and -down mutants of MoSET1-
 365 dependent TFs in *P. oryzae*. **a** Diameters of fungal colonies were measured at 9 days
 366 after inoculation on rich agar medium. **b** Conidiation was evaluated by counting the
 367 number of conidia under a light microscopy as described in details in Materials and
 368 methods. **c-d** The rates of conidial germination (**c**) and appressorium formation (**d**) were
 369 measured by observing conidial suspension on hydrophobic surface under a light
 370 microscope after 5 h (conidial germination) and 24 h (appressorium formation)
 371 incubation at 25°C.

372 Black bars indicate the wild-type strain Br48 (WT) and grey bars represent knock-out
 373 and -down mutants of MoSET1-dependent TFs and their gene complemented strains
 374 (c Δ mgg_04699 and c Δ mgg_06898). Data show fold change (relative to the wild-type
 375 strain) \pm standard error (n = 3). Different characters in the graphs indicate significant
 376 differences by Tukey's HSD ($p < 0.05$) ND, not determined.

377

378 **Fig. 4** Inoculation test of knock-out and -down mutants of MoSET1-dependent TFs in
 379 *P. oryzae*. **a** Infection assay was performed on the wheat cultivar Norin 4 at 23°C. Four
 380 to five days after inoculation, symptoms on the inoculated plants were evaluated. Letters

381 under pictures of infected leaves indicate disease index values by a grading method
382 (Hyon et al., 2012). This experiment was repeated at least three times, and
383 representative samples are presented. **b** The rates of infection hyphae formation in
384 infected leaves. The black bar indicates the wild-type strain Br48 (WT) and grey bars
385 represent knock-out and –down mutants of MoSET1-dependent TFs and a gene
386 complemented strain (cΔm_{gg_04699}). Error bars represent standard errors of the mean
387 (n = 10). Different characters in the graph indicate significant differences by Tukey's
388 HSD ($p < 0.05$).

389

390 **Fig. 5** Schematic diagram of putative MoSET1 regulatory network during infection-
391 related morphogenesis in *P. oryzae*.

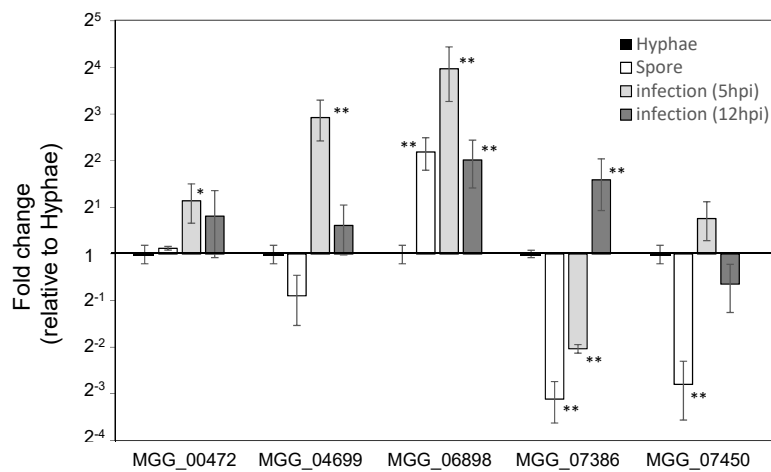


Fig 1. Quantitative RT-PCR analysis of five MoSET1-dependent transcription factors at hyphal, conidial and infectious stages in *P. oryzae*. Actin was used to normalize mRNA expression level. Data show fold change (relative to mRNA quantity in hyphae) \pm standard error (n = 3). Asterisks are given to indicate significant difference at p < 0.05 (*) and p < 0.01 (**) (two-tailed t-test).

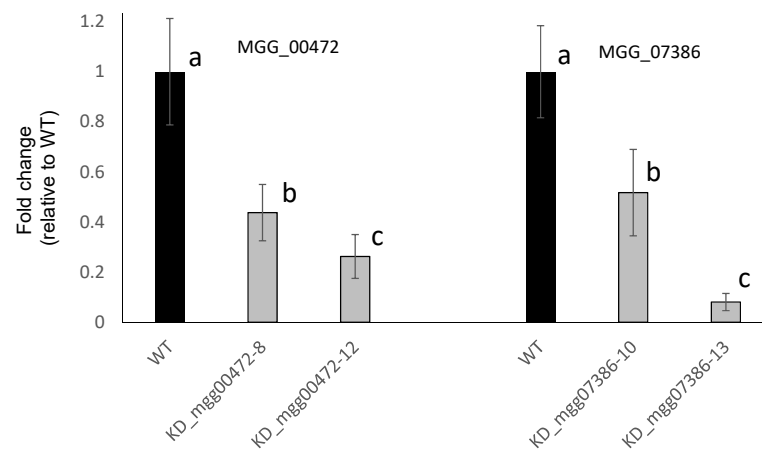


Fig 2. Quantitative RT-PCR analysis of MGG_00472 and MGG_07386 mRNA in candidates of their knock-down mutants. Actin was used to normalize mRNA expression level. Data show fold change (relative to mRNA quantity in the wild-type strain) \pm standard error (n = 3). a-c, Different characters indicate significant differences by Tukey's HSD (P < 0.05).

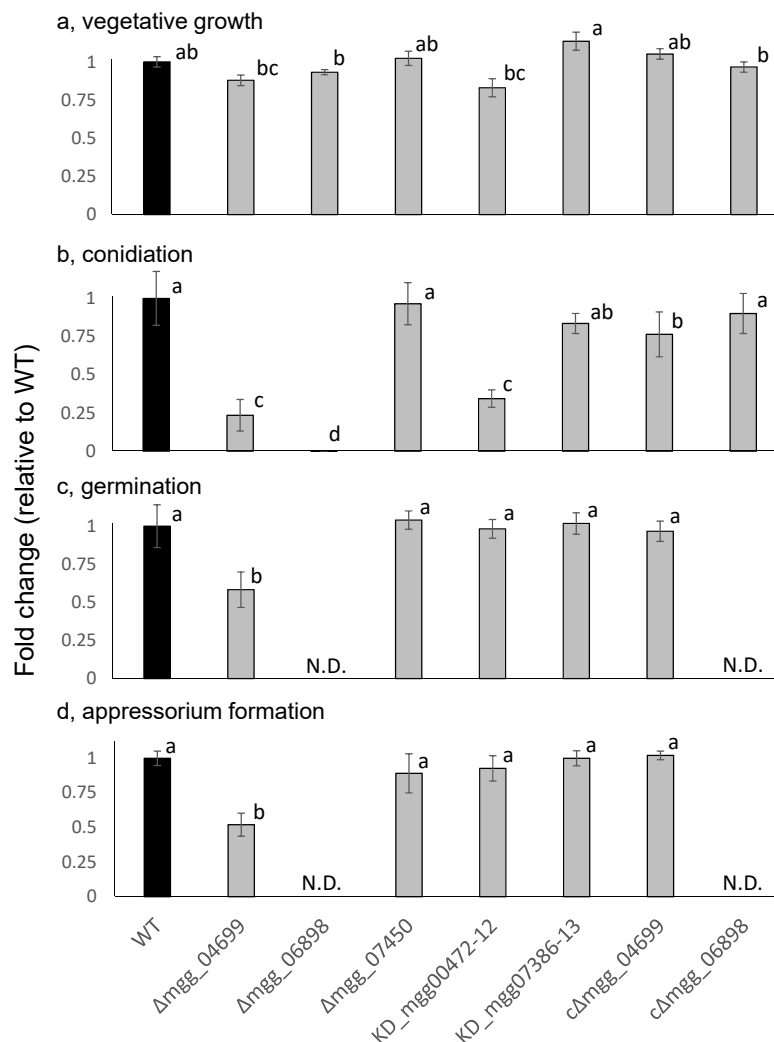


Fig 3. Phenotypic characterization of knock-out and -down mutants of MoSET1-dependent TFs in *P. oryzae*. **a**, Diameters of fungal colonies were measured at 9 days after inoculation on rich agar medium. **b**, Conidiation was evaluated by counting the number of conidia under a light microscopy as described in details in Materials and method. **c-d**, The rates of conidial germination (c) and appressorium formation (d) were measured by observing conidial suspension on hydrophobic surface under a light microscope after 5 h (conidial germination) and 24 h (appressorium formation) incubation at 25°C. Black bars indicate the wild-type strain Br48 (WT) and grey bars represent knock-out and -down mutants of MoSET1-dependent TFs and their gene complemented strains (cΔmgg_04699 and cΔmgg_06898). Data show fold change (relative to the wild-type strain) ± standard error (n = 3). a-d, Different characters in the graphs indicate significant differences by Tukey's HSD (P < 0.05). ND, not determined.

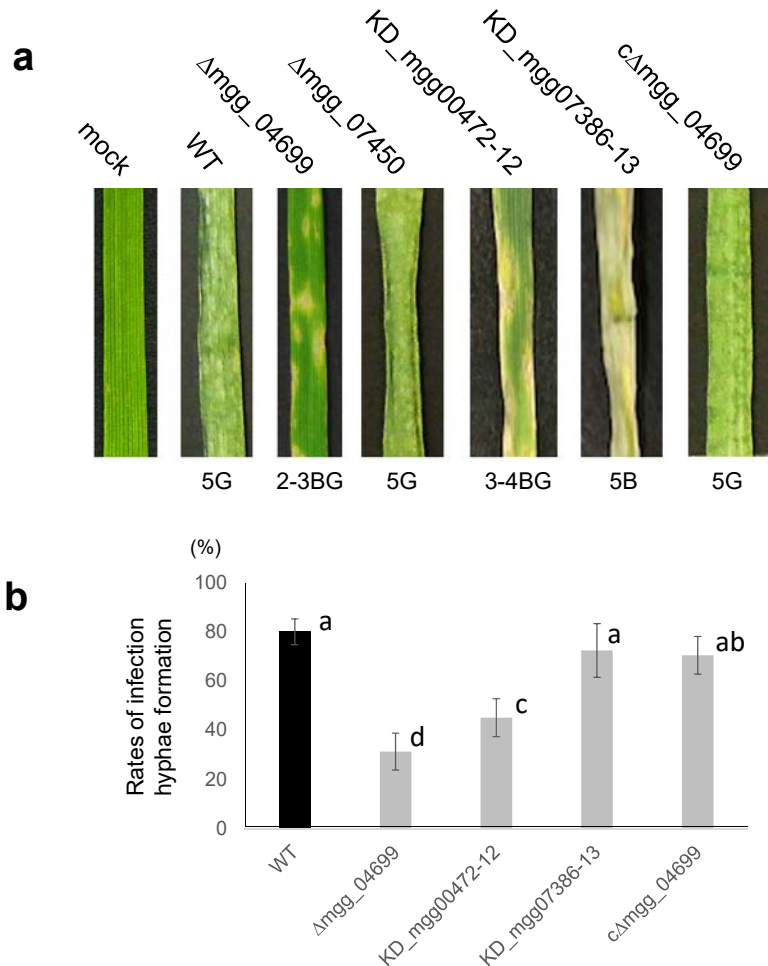


Fig. 4. Inoculation test of knock-out and -down mutants of MoSET1-dependent TFs in *P. oryzae*. **a**, Infection assay was performed on the wheat cultivar Norin 4 at 23°C. Four to five days after inoculation, symptoms on the inoculated plants were evaluated. Letters under pictures of infected leaves indicate disease index values by a grading method (Hyon et al., 2012). This experiment was repeated at least three times, and representative samples are presented. **b**, The rates of infection hyphae formation in infected leaves. The black bar indicates the wild-type strain Br48 (WT) and grey bars represent knock-out and – down mutants of MoSET1-dependent TFs and a gene complemented strain ($c\Delta mgg_04699$). Error bars represent standard errors of the mean ($n = 10$). a-d, Different characters in the graph indicate significant differences by Tukey's HSD ($P < 0.05$).

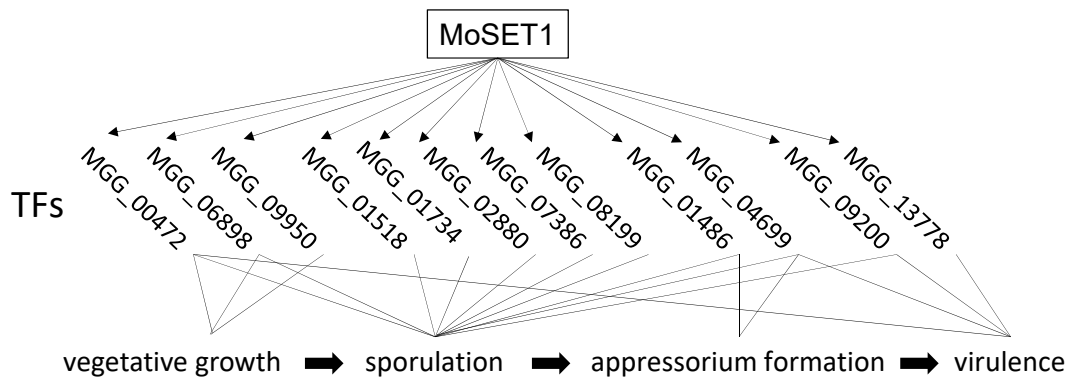


Fig. 5. Schematic diagram of putative MoSET1 regulatory network during infection-related morphogenesis in *P. oryzae*.